Applied Surface Science 638 (2023) 158062

Contents lists available at ScienceDirect

Applied Surface Science

journal homepage: www.elsevier.com/locate/apsusc

Full Length Article

Tuning the electrochemical response of PCL-PEDOT:PSS fibers-based sensors by gas dissolution foaming

Suset Barroso-Solares [a,b,c,*], Javier Pinto [a,b,c], Coral Salvo-Comino [b,d], Daniel Cuadra-Rodríguez [a], Cristina García-Cabezón [b,d], Miguel Angel Rodríguez-Pérez [a,b], Maria Luz Rodríguez-Méndez [b,d]

[a] Cellular Materials Laboratory (CellMat), Condensed Matter Physics, Crystallography, and Mineralogy Department, Faculty of Science, University of Valladolid, Spain
[b] BioEcoUVA Research Institute on Bioeconomy, University of Valladolid, Spain
[c] Study, Preservation, and Recovery of Archaeological, Historical and Environmental Heritage (AHMAT) Research Group, Condensed Matter Physics, Crystallography, and Mineralogy Department, Faculty of Science, University of Valladolid, Spain
[d] Group UVaSens, Escuela de Ingenierías Industriales, Universidad de Valladolid, Paseo del Cauce, 59, 47011 Valladolid, Spain

ARTICLE INFO

Keywords:
Electrospinning
Hollow fibers
CO_2 foaming
Catechol
Impedance

ABSTRACT

A new procedure to enhance the performance of polymer-based electrochemical sensors is proposed in this work. Polycaprolactone (PCL) electrospun fiber mats with tunable fiber morphology are functionalized with a conductive polymer (PEDOT:PSS) by a facile dip-coting process, providing them the necessary electrical conductivity to work as sensors. The modification of the fiber morphology is achieved by an enhanced gas dissolution foaming procedure, an environmentally friendly procedure that employs CO_2 as blowing agent and takes advantage of recent advances that allowed extending such procedure to polymeric microfibers. Thus, the enhanced gas dissolution foaming approach was employed both before and after the coating of the fiber mats with PEDOT:PSS, producing in both cases hollow fibers with enhanced surface porosity and area, as well as increased diameter regarding the initial solid PCL fibers. The addition of PEDOT:PSS, both in solid and foamed PCL fibers, allows their use as sensors, as proved by cyclic voltammetry in a KCl solution, as well as calibrated with catechol solutions. Remarkable influence of the foaming procedure on the performance of the sensors have been found, proving by a detailed characterization that the foaming procedure applied after the PEDOT:PSS coating provides an enhanced sensoring response (i.e., increased signal, optimal linearity, decreased LOD) due to their superior surface area and optimal PEDOT:PSS distribution along the fiber mats, not only covering the external surface of the fibers but infusing into the inner regions.

1. Introduction

Polycaprolactone (PCL, $(C_6H_{10}O_2)_n$), a well-known thermoplastic polyester-based polymer, is widely used in several applications by its unique properties. It can be highlighted the use of PCL in the biomedical field, in which this polymer is employed in scaffolds, surgical sutures, drug delivery, and wound dressing [1–4]. In addition to being nontoxic and biocompatible, PCL presents good mechanical properties, biodegradability, good solubility, blend compatibility, and low melting point. These interesting features made PCL also suitable for several other applications, such as in the textile industry [5], water treatment [6,7], or in the development of electronic [8,9] and electrochemical devices [10–12].

For most of these applications, PCL must be employed in a form exhibiting high porosity and the largest possible surface area. Such features can be easily achieved by the use of electrospun fibers mats [13]. Electrospinning is the most straightforward technique for producing polymeric fibers in a wide range of sizes from micro to nano scale, being useful in several applications [6,14]. In brief, this efficient and inexpensive technique is based on electrostatic forces, employing an electrical field to control the fibers formation from a polymeric solution [2]. By adjusting their fabrication parameters, electrospun fibers can be obtained with proper features for each target application [15]. Moreover, fine tuning of those properties can be archived by blending or by surface modification prior or after the electrospinning process, respectively.

* Corresponding author.
E-mail address: suset.barroso@uva.es (S. Barroso-Solares).

https://doi.org/10.1016/j.apsusc.2023.158062
Received 15 April 2023; Received in revised form 24 June 2023; Accepted 16 July 2023
Available online 17 July 2023

For instance, PCL fibers with enhanced properties have been successfully developed for water remediation. In this field [16,17]the fibers should work in an aqueous environment, generally under agitation, being important to consider the enhancement of the mechanical properties, aiming to avoid the disaggregation of the fiber mats and extending their durability [6]. [6,18]. Moreover, targeting biomedical applications it is possible to load or coat electrospun PCL fibers with active compounds, including conductive polymers such as polypyrrole (PPy), capable of increasing the biocompatibility of the fibers and helping in healing in a quicker time; in all the cases without giving up the good mechanical properties of the fibers [2,19,20].

The combination of PCL with conductive polymers is also essential to produce PCL-based fibers for electrochemical devices. In this field, PCL fiber mats can provide significant advantages such as mechanical strength, uniformity, tunable porosity, larger surface area, etc.[13]. However, an essential property for this type of application, electrical conductivity, is elusive for pristine PCL fiber mats [19]. Therefore, for sensing applications PCL needs to be blended or functionalized with other polymers to improve their conductivity or used as a host due to its ability to coordinate cations through its carbonyl group and Lewis base ester oxygen [4,20]. Several conductive polymers have proved to be suitable for the development of sensing applications, such as polyaniline (PANI), polypyrrole (PPy), polythiophene (PTh), poly(3,4-ethylenedioxythiophene):poly(styrene sulfonate) (PEDOT:PSS) [4,20–23]. Among them, it can be highlighted the PEDOT:PSS, which is nontoxic and biocompatible, and presents optimal chemical properties and thermal stability, as well as high electrical conductivity [24,25].

In particular, PEDOT:PSS-based fibers are commonly used in sensor development due to their high stability, taking advantage of the high surface area provided by the fiber mats porous structure [4,13,24,25]. PEDOT:PSS-based sensors can reach sensing properties similar to indium-tin oxide (ITO) electrodes, but being less expensive [26]. Aiming to achieve better electrochemical properties, PEDOT:PSS composite fibers have been obtained by incorporating different nanoparticles (NPs) such as Copper, graphene oxide (GO), carbon nanotubes (CNT), or titanium dioxide (TiO_2) is necessary to employ complex production routes to obtain PEDOT:PSS fibers (e.g., hydrothermal confinement reaction) [27,28], while their obtention through electrospinning is hindered by a poor solution processability and low viscosity [26]. To this aim, it is required to blend the PEDOT:PSS solutions with other polymers, such as polyvinyl alcohol (PVA or PVOH), or Poly-vinylpyrrolidone (PVP) [25,26,29]. Nevertheless, the current preparation process of these materials is relatively complex, and their complete potential has not been fully exploited [30], whereas some works also suggest coating procedures using PEDOT:PSS to functionalize polymeric fiber mats his polymer as coating layer is usually hindered by its tendency to present delamination induced by the swelling of PSS in presence of water [31].

As far as we know, no previous works have explored the combination of electrospun PCL fibers with PEDOT:PSS aiming to produce electrochemical devices, although previous evidence suggest that PCL and PEDOT:PSS may present adequate compatibility. In fact, PCL nanofibers have been used as a binder to adhere a PEDOT:PSS/CNT coating to a thermoplastic Polyurethane (PU) through a complex process capable of producing strain sensors [32]. Also, Ferlauto et al.[30] reported the fabrication of transient neural probes that can monitor brain activity in mice for a few months, created from the encapsulation of PEDOT:PSS doped with ethylene glycol between different layers of PCL. It is possible also to obtain multifunctional micro/nanofibrous scaffolds with biomimetic architectures, electrical conductivity, and even biosensing properties for the cardiac regeneration form melt-based electrohydrodynamic printing techniques, combining 3D printed PCL fibers and PEDOT:PSS-PEO sub-microfibers [33]. Moreover, the functionalization of PCL scaffolds with PEDOT has also been studied demonstrating that the combination of both polymers can produce electroactive scaffolds for regenerative medicine [28,34].

The last two approaches are based on the successful functionalization of porous PCL substrates (e.g., 3D printed fibers and scaffolds) with PEDOT:PSS. Therefore, extending the functionalization approach with PEDOT:PSS to electrospun PCL fibers could take advantage of the tunable porous morphology that this fabrication technique can provide. Moreover, recent advances proved that it is possible to increase the electrospun PCL fibers surface area and tune their morphology by an easy and environmentally friendly enhanced gas dissolution foaming approach [2].

In brief, the gas dissolution foaming technique consists of dissolving pressurized CO_2 (principally, it is also possible to use N_2) into a polymer matrix, and by controlling the saturation pressure, time, and temperature it is possible to induce and control the formation of pores once the pressure is released [2,26]. The fine tuning of the electrospun PCL fibers surface area and porosity provided by this technique has shown a remarkable influence on their performance on drug delivery [2], while their potential in other applications such as sensoring is still unknown. It should be noted that the gas dissolution foaming approach is a simple and environmentally friendly procedure to obtain porous polymers, which has been recently adapted to produce hollow polymeric fibers, becoming a straightforward and simple approach with the potential to outperform other techniques such as co-extrusion/co-axial spinning/electrospinning, template method, 3D printing, or self-crimping [35].

In this study, the potential for sensoring applications of the enhanced surface area and tunable porous morphology provided by the foaming of electrospun PCL fibers is evaluated. With this aim, electrospun PCL fibers with a precise and independent control of their morphology, provided by the enhanced gas dissolution foaming route, have been functionalized with PEDOT:PSS for the first time. In particular, four different sensors were developed, by tuning the morphology of the fibers as well as incorporating the PEDOT:PSS coating at different stages of the production routes, aiming to identify the optimal production route and fiber morphology to improve their electrochemical response. Electrochemical impedance spectroscopy (EIS) was used to characterize the voltammetric sensors. The electrochemical response of the sensors has been evaluated in a reference KCl solution. Also, the sensors proved to be efficient in the detection of catechol, a polyphenol, which is a typical polymer in wine quality control. While the sensitivity and detection limit of this sensors was evaluated by cyclic voltammetry. Finally, the detailed characterization and analysis of the performance of the sensors proved that the sensors with enhance surface area and porosity provided by the gas dissolution foaming approach achieved a remarkable sensoring performance in comparison with the initial solid fibers.

2. Experimental section

2.1. Materials

Polycaprolactone (PCL, M_n: 80 000, $\rho = 1.15$ g/cm^3, melting point (T_m) = 60 °C), poly(3,4-ethylenedioxythiophene)-poly (styrenesulfonate) (PEDOT:PSS, 3.0–4.0 v.t% in H_2O, high-conductivity grade), potassium chloride (KCl), and pyrocatechol, were purchased from Sigma-Aldrich (Madrid, Spain). Poly (vinyl alcohol) (PVOH) (Mowiflex C17, $\rho = 1.25$ g/cm^3, glass transition temperature (T_g) = 60 °C, T_m = 170 °C) was gently provided by Kuraray (Frankfurt, Germany). Chloroform was purchased from Scharlab (Barcelona, Spain). Deionized water was employed in all the tests using Milli Q water (resistivity 18.2 MΩ•cm), and a medical-grade carbon dioxide (CO_2) presenting 99.9 % purity was employed in the foaming processes.

Indium tin oxide (ITO) glass substrates purchased from Sigma-Aldrich (Darmstadt, Germany) were used as support to provide a rigid structure to the samples.

2.2. Preparation of PCL-PEDOT:PSS sensors

Fig. 1 summarizes the steps followed to fabricate the four different sensors which were designed and tested in this work. The common step

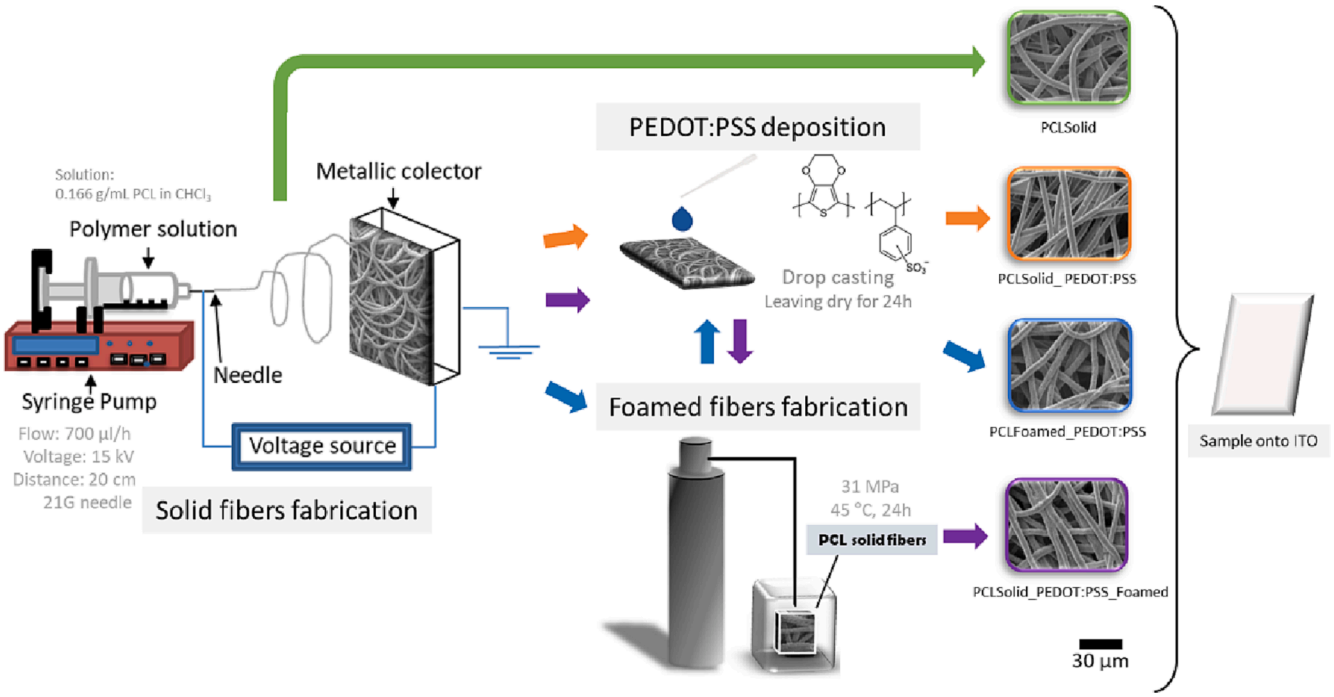

Fig. 1. Schematic representation of the fabrication of PCL-PEDOT:PSS sensors (common scale bar for the four SEM micrographs of the sensors surface can be found below the micrographs).

in the manufacture of these sensors is the initial fabrication step of the polymeric-base fibers mats. The PCL solid fiber mats were fabricated by a conventional horizontal electrospinning process. 1 mL of 0.166 mg/L PCL solution in Chloroform was transferred into a syringe which was placed in a syringe pump (NE-1000, New Era Pump Systems, Inc.) providing a flow rate of 0.7 mL/h. The solid fibers were collected in a copper target covered with aluminium foil placed at 20 cm from the needle (21G) using a fixed voltage at 15 kV, at room temperature (RT) and ambient humidity about 30 %. The obtained fiber mats present thicknesses of about 200 µm.

The electrospun solid fibers without further modification were employed as the first sensor, and from now on, this sensor will be referred as PCLSolid sensor.

The second sensor were obtained by coating the fiber mats with a thin layer of conductive polymer PEDOT:PSS using a drop casting method. A drop of the PEDOT:PSS solution was deposited on the fibers (1 mL of solution by each mg of fibers to ensure to have an homogeneous layer). This sensor will be referred as PCLSolid_PEDOT:PSS.

A more complex manufacturing process was carried out to obtain sensors 3 and 4, where in addition to the deposition of a thin layer of PEDOT:PSS, the samples were foamed. Foaming experiments were performed according to the gas dissolution foaming process using carbon dioxide (CO_2) as a blowing agent, [36,37] following the methodology described in a previous work [2]. In brief, before the foaming process, the samples were coated by immersing them in a PVOH solution in water (5 wt.%) and then dried overnight at RT, obtaining a 200 µm of solid PVOH film in which the solid fiber mats were completed imbibed. It is important to point out that PVOH is employed as a gas diffusion barrier, without which the foaming in micrometric fibers cannot be accomplished. Then, the samples were introduced into a pressure vessel (PARR 4760 model, Moline, IL, USA), and kept for 20 h in a CO_2 atmosphere at 30 MPa and 45 °C using a gas pump (STF-10 model provided by Supercritical Fluid Technologies Inc., Newark, DE, USA) and a temperature controlled (CAL 3300). Then the pressure was quickly released, and the samples were extracted from the vessel. In the case of the third sensor, the samples were first foamed and then coated with PEDOT:PSS, following the same procedure described for the solid PCL fiber mats, and from now on they will be referred as PCLFoamed_PEDOT:PSS. On the contrary, the last sensor was obtained by performing the foaming procedure after being coated with PEDOT:PSS. This sensor will be described as PCLSolid_PEDOT:PSS_Foamed. In all the cases, after the foaming procedure the samples were introduced in an ultrasonic hot water bath at 25 °C for 3 cycles of 20 min each to ensure the complete removal of the PVOH layer. Finally, all the samples (approximately 1x2 cm^2) were attached with double-sided tape with the same dimensions of the sample on slightly larger Indium tin oxide (ITO) sheets to provide mechanical support prior to their characterization as sensors.

2.3. Characterization

The microstructure and morphology of the fibers were studied through Scanning Electron Microscopy (SEM) (HITACHI FlexSEM 1000) after being coated with gold nanoparticles. The diameter distribution of the fiber mats was obtained by measuring at least 100 individual fibers by image analysis software FIJI/ImageJ [38]. In addition, the distribution of the layer of PEDOT:PSS deposited on the fibers were studied using SEM coupled to energy dispersive spectroscopy (SEM-EDS) without any coating (ESEM FEI - Quanta 200FEG).

Raman spectroscopy, in microscopy mode, was performed on the surface of the different sensors, using a portable BWTEK Raman spectrometer equipped with a microscopy head BAC151C-785, BWTEK Exemplar-PRO (CCD BTC675N) detector, and using an excitation wavelength of 785 nm.

The amount of PEDOT:PSS deposited in the different sensors were determined by two methods and quantified by the corresponding mass increase percentage (Δwt.%) of the sensors. First, it was determined by weighing the samples before and after the coating process, determining the mass increase of the entire sensor with respect to the initial mass. Second, the amount of PEDOT:PSS transferred to the sensors was estimated from the weight loss related to the PEDOT:PSS measured by Thermogravimetric Analysis (TGA) (SDTA851, Mettler Toledo). In this analysis the samples were heated from 50 to 800 °C (10 °C/min) in a nitrogen atmosphere. Typically, PEDOT:PSS thermograms show three decomposition stages: the first stage is the water and moisture

evaporation (50–180 °C temperature range); the second stage is the decomposition of PSS (by the rupture of the sulfonate group from styrene at 180–400 °C); and the last stage is found at a temperature range of 400–790 °C is due to the decomposition of PEDOT (main chain) [39–41]. While PCL decomposes in a unique stage around 400 °C [42]. Therefore, it is possible to estimate the amount of PEDOT:PSS from the decomposition of PSS between 180 and 400 °C.

The surface area of the sensors was measured by BET using a Surface Area and Porosity Analyzer ASAP 2420 (Micromeritics Instrument Corp., Norcross, GA, USA).

Electrochemical impedance spectroscopy (EIS) can provide information about the conductivity changes resulting from the incorporation of PEDOT:PSS into PCL fibers. EIS was performed using a potentiostat/galvanostat (PARSTAT 273A, Princeton Applied Research, Princeton, NJ, USA) and an impedance analyzer (Solartron SI 1260, Solartron Analytical, Farnborough, UK). The measurements were carried out in a 0.1 M KCl solution, 10 mV amplitude, 0.1 V working potential, and frequency range from 0 to 100 kHz. The impedance response was fitted with Zview2 software obtaining the Nyquist and Bode diagrams.

The resistance to the solution (R_s), the constant phase element (CPE), and the electrical resistance in parallel (R_{ct}), which is the resistance to electron transfer, were studied. The impedance (Z) of the constant phase element CPE is defined by the Equation (1)

$$Z = \frac{1}{C_{CPE}(jw)\alpha_{CPE}} \quad [1]$$

where C is the capacitance, ω is the angular frequency, and α is the coefficient indicating the deviation from an ideal capacitor.

Finally, cyclic voltammetry was performed in a PGSTAT128 potentiostat/galvanostat (AutolabMetrohm, Utrecht, The Netherlands) controlled by the CView software at RT. The three-electrode cell of 40 mL is composed of a platinum plate as a counter electrode (CE) (2 cm^2 of active surface, which was flamed before to use), an Ag/AgCl as reference electrode (RE) and the developed polymeric sensors as working electrode (WE). The electrochemical response of the conductive polymer-based sensors was studied from −1.0 to + 1.2 V (vs Ag/AgCl (1 M KCl)) at a scan rate 100 mV/s. 10 cycles for each sample deposited in ITO were carried out for this study in 0.1 M of KCl. Also, calibration curves were obtained from catechol solutions with concentrations ranging from $1{\cdot}10^{-5}$ to $1{\cdot}10^{-3}$ M. The limits of detection (LODs) were calculate following the 3σ/m criterion, where σ is the standard deviation of 3 different blanks and m is the slope of the calibration plot.

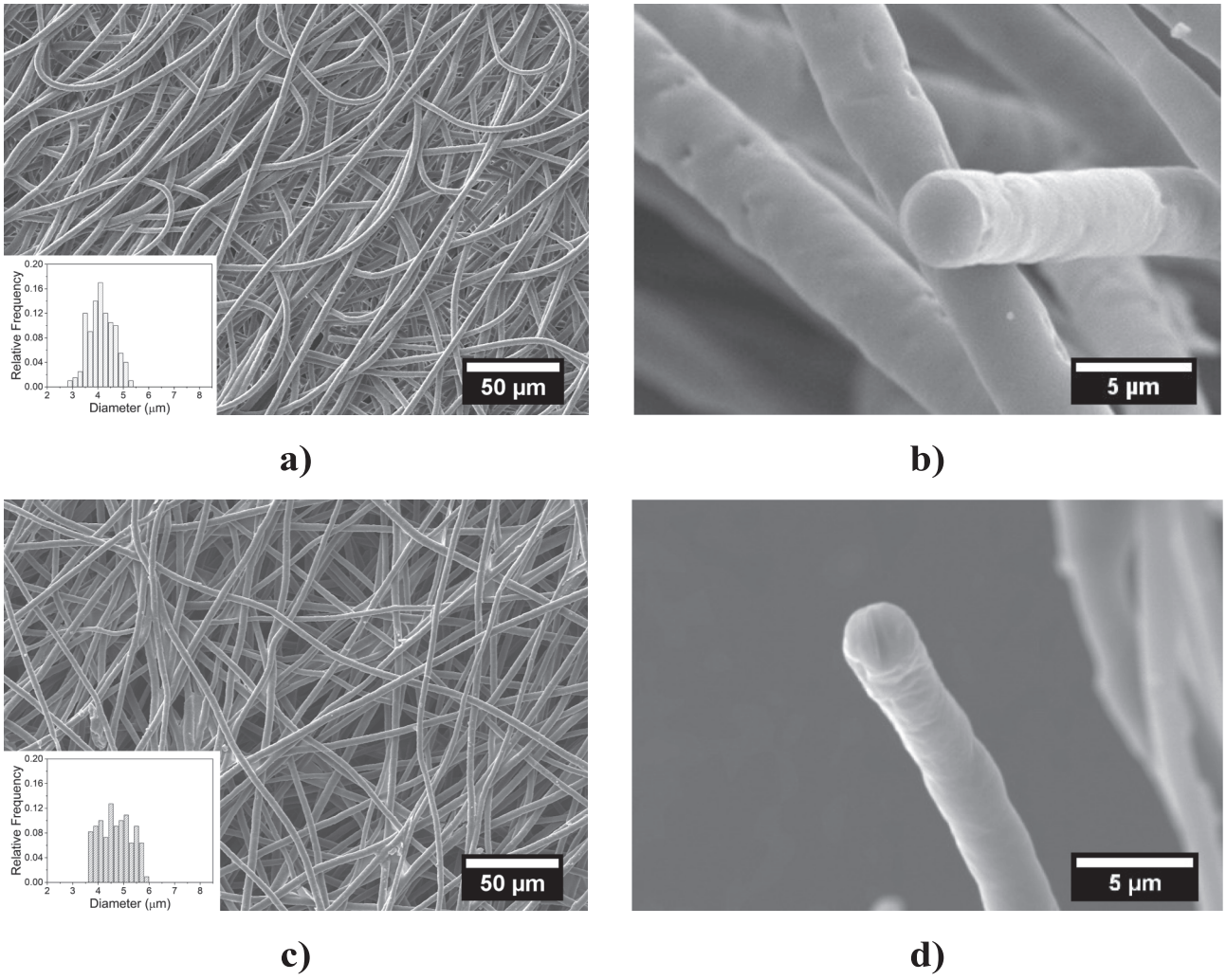

Fig. 2. SEM micrographs of the surface (including the diameter histogram as inset) **(a)** and cross-section **(b)** of the PCLSolid sensor, as well as of the surface (including the diameter histogram as inset) **(c)** and cross-section **(d)** of the PCLSolid_PEDOT:PSS sensors.

3. Results and discussion

3.1. Sensors characterization

PCL solid fiber mats obtained by electrospinning were studied by SEM (Fig. 2). The fiber mats present a relatively homogeneous diameter distribution, showing an average value of 4.14 ± 0.51 μm (Fig. 2**a**). In a close-up micrograph (Fig. 2**b**), it can be observed that these fibers present a quite smooth surface. Also, the cross-section of the individual fibers shows that they are solid (Fig. 2**b**) [43]. Moreover, the solid PCL fiber mats presented a BET surface area of 4.35 m^2/g.

It should be noted that PCL is not a conductive polymer, so it cannot be successfully used for sensor development by itself [9]. After the PEDOT:PSS coating on the solid fibers (PCLSolid) the morphology of the fibers or their porosity is not significantly modified (Fig. 2**c and 2d).** The average diameter of the coated fibers, PCLSolid_PEDOT:PSS, slightly increases to 4.68 ± 0.61 μm, indicating that a thin PEDOT:PSS coating of only hundreds of nanometers has been achieved, whereas their surface area increases by 20 % (5.21 m^2/g) probably related to the presence of bridges between the fibers **(**see Supporting Information, **Fig. S1**). Again, the cross-section of individual fibers shows that they are still solid **(**Fig. 2**d)** [43].Therefore, the addition of PEDOT:PSS following the proposed procedure proved not to significantly modify the morphology of the PCL fiber mats. This is a desired feature (i.e., the objective is taking advantage of the fibers morphology), but also it is required to prove a proper presence and homogeneous distribution of the PEDOT:PSS on the fibers mats. The presence of PEDOT:PSS on the surface of the PCLSolid_PEDOT:PSS fibers was proved by the detection of Sulfur (S) at the surface of the fibers by SEM-EDS, an element not related neither detected in pristine PCL fibers (see Supporting Information, **Fig. S2**) [44,45]. Thus, the obtained results confirmed a proper distribution of the PEDOT:PSS coating the PCL fibers without modifying or hindering their morphology, a feature that allows taking advantage of both the conductivity of PEDOT:PSS and the morphology of the PCL fibers.

On the contrary, the morphology of the fibers noticeable changed after the foaming process. Fig. 3 shown a clearly increased surface porosity for PCLFoamed_PEDOT:PSS sensors and PCLSolid_PEDOT:PSS_Foamed sensors (Fig. 3**a and 3.c**), regarding both the PCLSolid and PCLSolid_PEDOT:PSS sensors. Moreover, the most characteristic feature of the foamed samples is the apparition of inner porosity leading to hollow structures (Fig. 3**b and 3d**). Accordingly, the expanded fibers present increased diameters (see insets in Fig. 3**a and 3c**) of about 5.27 ± 0.72 μm and 5.14 ± 0.63 μm, respectively for fiber mats foamed before and after the coating with PEDOT:PSS. It should be noticed that the application of the PEDOT:PSS layer before the foaming procedure does not affects the expansion of the fibers due to the foaming procedure.

Moreover, the increased porosity of the foamed fibers was further confirmed by BET measurements. The PCLFoamed_PEDOT:PSS samples presented a BET surface area of 11.86 m^2/g, whereas the

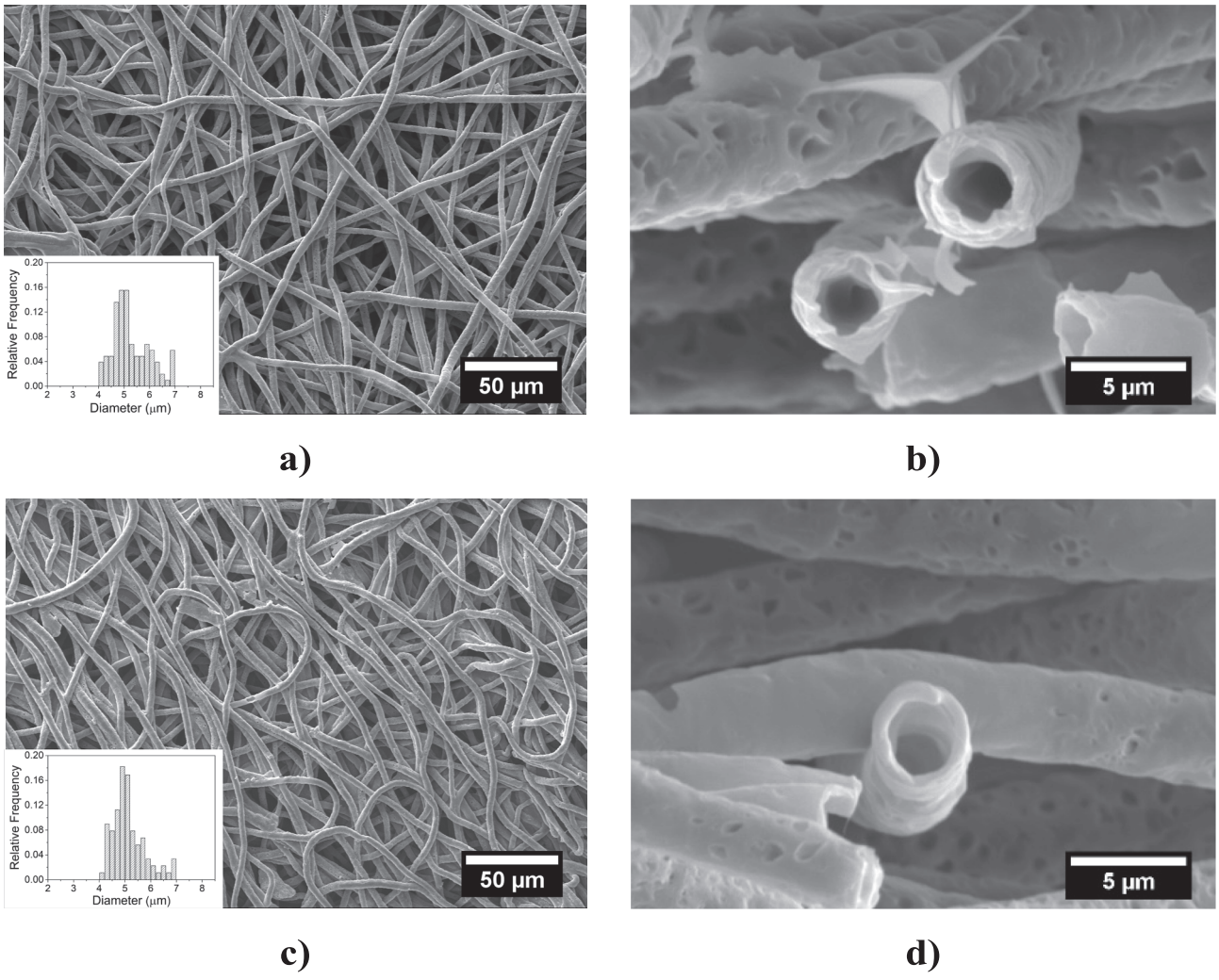

Fig. 3. SEM micrographs of the surface (including the diameter histogram as inset) **(a)** and cross-section **(b)** of the PCLFoamed_PEDOT:PSS sensors, as well as of the surface (including the diameter histogram as inset) **(c)** and cross-section **(d)** of the PCLSolid_PEDOT:PSS_Foamed sensors.

PCLSolid_PEDOT:PSS_Foamed samples presented a BET surface area of 26.96 m^2/g. Therefore, the foaming process is capable of increasing the BET surface area of the fibers more than 5 times. Although it should be noted that by applying the coating once the fibers have been foamed, the surface area only increases 2 times. This behavior can be justified by the fact that by covering the fibers once foamed, part of the surface porosity achieved in the foaming process is lost below the coating layer.

Also, it has been possible to identify the presence of PEDOT:PSS on the surface of the foamed sensors by identifying the presence of sulfur atoms on its surface by SEM-EDS (see Supporting information, section S2), verifying that the homogeneity of the coating is maintained even when the PEDOT:PSS coated PCL fibers are subjected to the foaming process. Moreover, to check if during the foaming process it was possible to transfer part of the PEDOT:PSS to the interior of the fibers, SEM-EDS of cross-sections of the hollow fibers of the foamed sensors was performed. As it is shown in Fig. 4, the presence of sulfur atoms on the inner porosity of the hollow fibers is only verified in the PCLSolid_PEDOT:PSS_Foamed sensors. During the foaming process, the PCL is expected to reach its effective melting temperature (i.e., the depleted melting temperature due to the CO_2 plasticization [46]); therefore, the externally deposited PEDOT:PSS layer on the PCLSolid_PEDOT:PSS_Foamed sensors can be partially infused into the inner regions of the resulting hollow fibers. On the contrary, the coating of already foamed PCL fibers in the PCLfoamed_PEDOT:PSS sensors does not provide any mechanism for the PEDOT:PSS to reach the inner porosity of the hollow fibers.

The homogeneity of the PEDOT:PSS coating of the fibers on the different sensors was further studied by means of Raman spectroscopy in microscopic mode (Fig. 5**a**). It was found that the characteristic Raman peaks of the PCL could only be observed in the PCLSolid sensor, while in the rest of the sensors it was only possible to observe the characteristic Raman peaks of the PEDOT:PSS, regardless of the fiber or area under study in each sensor. The principal PCL Raman peaks or bands appears in the PCLSolid sensor located at 1720 1/cm (related to C = O stretching mode); groups of bands at 1465, 1440, and 1416 1/cm (CH_2 groups scissor vibration); bands at 1300 and 1280 1/cm (CH_2 groups wagging vibration); bands at 1040, 1110, and 1065 1/cm, (belonged to symmetric stretching of the C-O-C bond in the ester group of PCL), and at 912 1/cm (C-COO scissoring) in agreement to the literature [47,48]. In the rest of the sensors, the presence of PEDOT:PSS is evidenced by a strong band around 1400 1/cm ($C_\alpha = C_\beta$ symmetric stretching vibration), other bands at 1240 and 1360 1/cm, (C_α-C_α inter-ring stretching vibrations and the C_β-C_β stretching, respectively), while the vibrational modes located at 1100 and 980 1/cm correspond to the vibrational modes of PSS, and the bands at 984, 850 and 570 1/cm to the oxyethylene ring deformation-vibrations. Finally, another significant band appeared at 430 1/cm, corresponding to PEDOT doping by the SO_3^- ion from PSS units [49,50]. A detailed comparison of the main Raman band around 1400 1/cm of the PEDOT:PSS coatings with those of a self-standing PEDOT:PSS film evidenced a shift of the maximum from around 1420 1/cm in neat PEDOT:PSS to 1416 1/cm in both kinds of foamed fibers and 1406 1/cm in the solid fibers (Fig. 5**b**). This behavior suggests the existence of interaction between the PEDOT:PSS coating and the PCL fibers, as shifts on this PEDOT:PSS band have been previously related to interactions of the aromatic rings with other substrates or fillers [51].

Once the morphology of the fibers and the presence of PEDOT:PSS were addressed, the different sensors were characterized in terms of the amount of PEDOT:PSS incorporated. Table 1 summarizes the data obtained by two different methods, weight increase and TGA (see Experimental section). A reasonable agreement was found between the two techniques, confirming that there is a remarkable transfer of PEDOT:PSS to the sensors studied in this project. As expected, PCLSolid_PEDOT:PSS and PCLSolid_PEDOT:PSS_Foamed sensors presented the same amount of PEDOT:PSS transferred, about 20–25 wt.%. On the contrary, the PCLFoamed_PEDOT:PSS sensor reached a significantly higher amount of PEDOT:PSS, up to about 35–40 wt.%, by covering the larger surface area presented by the foamed PCL fibers.

3.2. Electrochemical properties

Once the features of the developed fibers mats were studied in detail, they were incorporated into an ITO substrate for their electrochemical characterization.

3.2.1. Electrochemical impedance spectroscopy (EIS)

Electrochemical impedance spectroscopy (EIS) has been used successfully to investigate the changes in conductivity caused by the introduction of PEDOT:PSS in voltammetric electrodes [52]. In this work, it has been applied to solid and hollow PCL fibers modified with PEDOT:PSS.

Fig. 6 shows the Nyquist and Bode diagrams for three types of electrodes: solid fibers coated with PEDOT:PSS:PCLSolid_PEDOT:PSS, PCLFoamed_PEDOT:PSS, and PCLSolid_PEDOT:PSS_Foamed.

In the Nyquist diagram (Fig. 6**a**), it can be observed an incomplete semicircle for all sensors, whose diameters, equivalent to the resistance to electron transfer, are clearly different in the three samples. The PCLFoamed_PEDOT:PSS is the one that presents clearly lower electronic resistance and, on the contrary, the PCLSolid_PEDOT:PSS is the one that presents the highest resistance. In the Bode diagram (Fig. 6**b**) it is clearly observed two-time constants: (i) the high-frequency region corresponding to the resistance of the solution that is similar in the three samples and (ii) followed by a linear behaviour indicating a combination of capacitance and resistance at the interface between the electrode and the solution. The impedance module in the low-frequency region is clearly higher for PCLSolid_PEDOT:PSS; on the contrary, PCLFoamed_PEDOT:PSS is the one that presents an impedance modulus several orders of magnitude lower. However, PCLSolid_PEDOT:PSS_Foamed presents an intermediate impedance module, which coincides with an intermediate resistance to electronic transfer.

Table 2 summarizes the quantitative values from a fit of the EIS spectra to equivalent circuits using Randel's electrical circuit, Fig. 6**c**. The resistance to the solution (R_s), a constant phase element (CPE), and

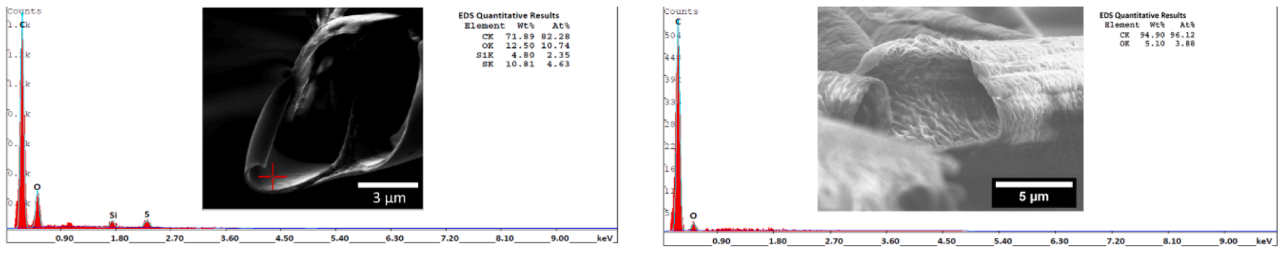

Fig. 4. SEM micrographs and EDS spectrums (Carbon (C), Oxygen (O), Sulfur (S)) of the cross-section of PCLSolid_PEDOT:PSS_Foamed **(a)** and PCLFoamed_PEDOT:PSS sensors **(b)**.

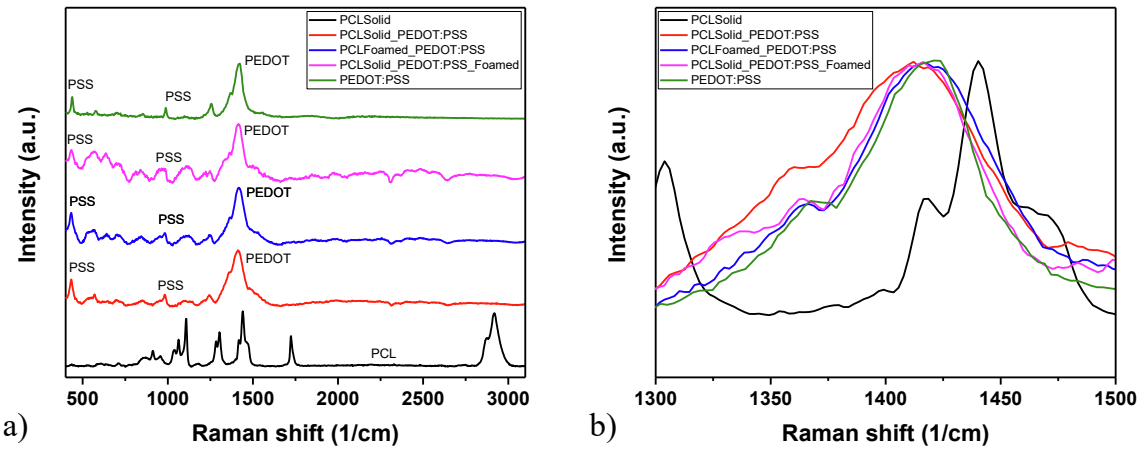

Fig. 5. Representative Raman spectra of the surface of the fibers of each of the sensors developed, showing the spectra of the PCL (PCLSolid), the PEDOT:PSS (PCLSolid_PEDOT:PSS, PCLFoamed_PEDOT:PSS and PCLSolid_PEDOT:PSS_Foamed) **(a)**, as well as a self-standing PEDOT:PSS film for comparison purposes. Detail of the 1300–1500 1/cm range **(b)**.

Table 1
Percentage by mass of PEDOT:PSS deposited in the different sensors determined by weighing the sensors before and after the coating procedure (mass increase) and TGA.

Sensors	Mass increase (Δwt.%)	TGA (Δwt.%)
PCLSolid	0	0
PCLSolid_PEDOT:PSS	20.50 ± 3.58	20.81 ± 1.01
PCLFoamed_PEDOT:PSS	35.39 ± 6.15	41.57 ± 0.95
PCLSolid_PEDOT:PSS_Foamed	25.92 ± 3.34	22.29 ± 1.23

an electrical resistance in parallel (R_{ct}), which is the resistance to electron transfer, was observed. The fit to the circuit is quite good in all cases, obtaining χ^2 values less than 10^{-3} in all cases.

The results indicate that the foaming processes clearly modifies the effect of PEDOT:PSS on the electrical behaviour of the sensors. The PEDOT:PSS deposited on the surface of the foamed fiber adheres much better than on the solid fiber and is capable of diffusing through the pores when the foaming process is performed after the PEDOT:PSS

Table 2
Results obtained from the impedance spectroscopy measurements.

Samples	R_s (Ω/cm^2)	C_{CPE} (μF)	α_{CPE}	R_{ct} (Ω/cm^2)
PCLSolid_PEDOT:PSS	89.7	2.59	0.87	1.6 E14
PCLFoamed_PEDOT:PSS	71.5	31.9	0.72	1.7 E4
PCLSolid_PEDOT:PSS_Foamed	64.5	6.93	0.82	2.6 E6

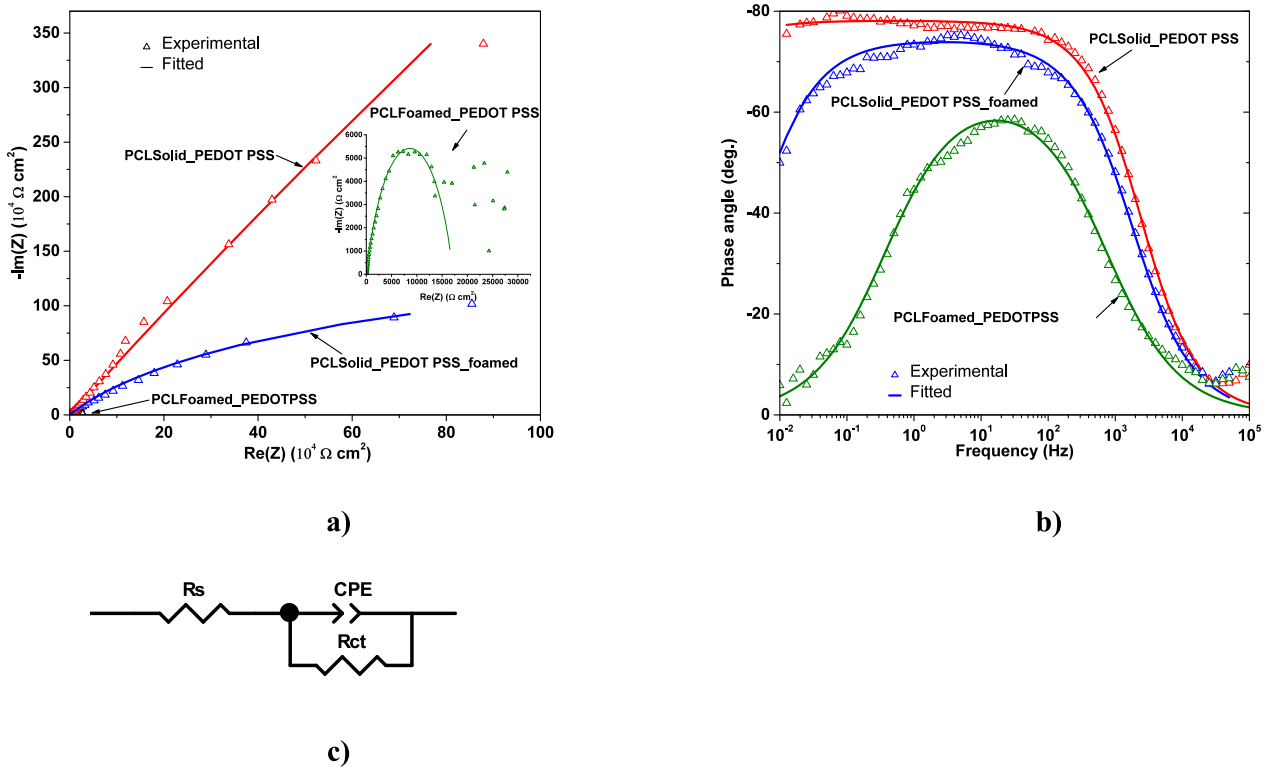

Fig. 6. Nyquist **(a)** and Bode **(b)** diagrams of the different sensors coated with PEDOT: PSS, PCLSolid_PEDOT:PSS, PCLFoamed_PEDOT:PSS, and PCLSolid_PEDOT: PSS_Foamed. Equivalent circuit **(c)**.

coating, as previously demonstrated, which makes the electronic resistance and the impedance modulus clearly lower than that observed in the PCLSolid_PEDOT:PSS. Further the differences between PCLSolid_PEDOT:PSS and PCLSolid_PEDOT:PSS_foamed intelligibly indicate that the foaming process clearly modifies the electrical behaviour of the fiber, achieving a significant decrease in the resistance to electronic transfer making it the best candidate for voltammetric sensors [53].

3.2.1.1. Cyclic voltammetry. The developed sensors were characterized by cyclic voltammetry (CV). Fig. 7 shows the cyclic voltammograms of the different sensors in 0.1 mol/L KCl solution after 10 cycles (the results of the ten consecutive measurements showed a coefficient of variation lower than 3 % in all cases between the first and the tenth cycle, see Supporting Information, Fig. S8d). The response of ITO glass is not shown in the Fig. 7 due to its low intensity. Under these conditions (ranging from −1.00 to + 1.20 V (vs Ag/AgCl) at scan rate 100 m/Vs), the uncoated fibers of PCL show an ohmic or linear behavior, just as expected (Fig. 7**a**). However, the rest of the sensors, which all have a PEDOT:PSS coating, showed the typical PEDOT:PSS response in both anodic and cathodic scans [54–56], in which the peak positions are not significantly modified after 10 cycles. In the case of the PCLSolid_PEDOT:PSS sensors (Fig. 7**b**), an oxidation peak appears around 0.30 V, whereas in the reduction region the peak is placed around −0.15 V which corresponds to the PEDOT:PSS response [54–56].

As abovementioned, the foaming process of the sensors leads to a greater surface area and porosity compared to the PCLSolid_PEDOT:PSS sensor. The enhanced surface area and porosity allow a higher active area of the PEDOT:PSS, which is directly reflected in a better electrochemical response of theses sensors, whose conductive polymeric coating facilitates the electron transference to the electrode surface, increasing the current intensity. Also, as the deposited PEDOT:PSS amount on the sensor increases for the PCLFoamed_PEDOT:PSS sensor (Δwt.%, see Table 1), the voltammetric behavior changes in both current and potential peak position as well as its shape. In this case, the increment in the peak current appreciated in Fig. 7**c** response indicates the larger PEDOT:PSS amount deposited onto the electrode surface with an enhanced surface area, increasing by this way the number of electroactive sites. On the contrary, the PCLSolid_PEDOT:PSS_Foamed sensor benefits from a higher enhancement of the surface area, but also for an improved distribution of the conductive PEDOT:PSS, not limited to the external surfaces but also to the inner porosity, providing also an improved response (Fig. 7**d**). In any case, the bundling created by the capillary forces during the immersion of the sensors in the solution leads to an enhancement mechanism, creating a better fiber-to-fiber contact. So, it is found that the greater surface area and porosity achieved in the foamed fibers, which allows the incorporation and good distribution of PEDOT:PSS, is directly reflected in a better electrochemical response of the sensors. In particular, it should be highlighted that, for the same amount of PEDOT:PSS transferred, the PCLSolid_PEDOT:PSS_Foamed sensors present a significantly enhance response regarding the PCLSolid_PEDOT:PSS sensor, proving the efficiency of the proposed foaming approach to develop electrochemical devices.

Additionally, the catalytic and sensing properties were studied by making controlled additions of catechol (10^{-4} M catechol solution in 0.1 M KCl, from 200 to 7500 μM), the resulting linear adjustment of each sensor can be observed in Fig. 8. The experiments were performed in the same range used to perform the CV (-1 to 1.2 V) at a rate of 100 mV/s (vs Ag/AgCl).

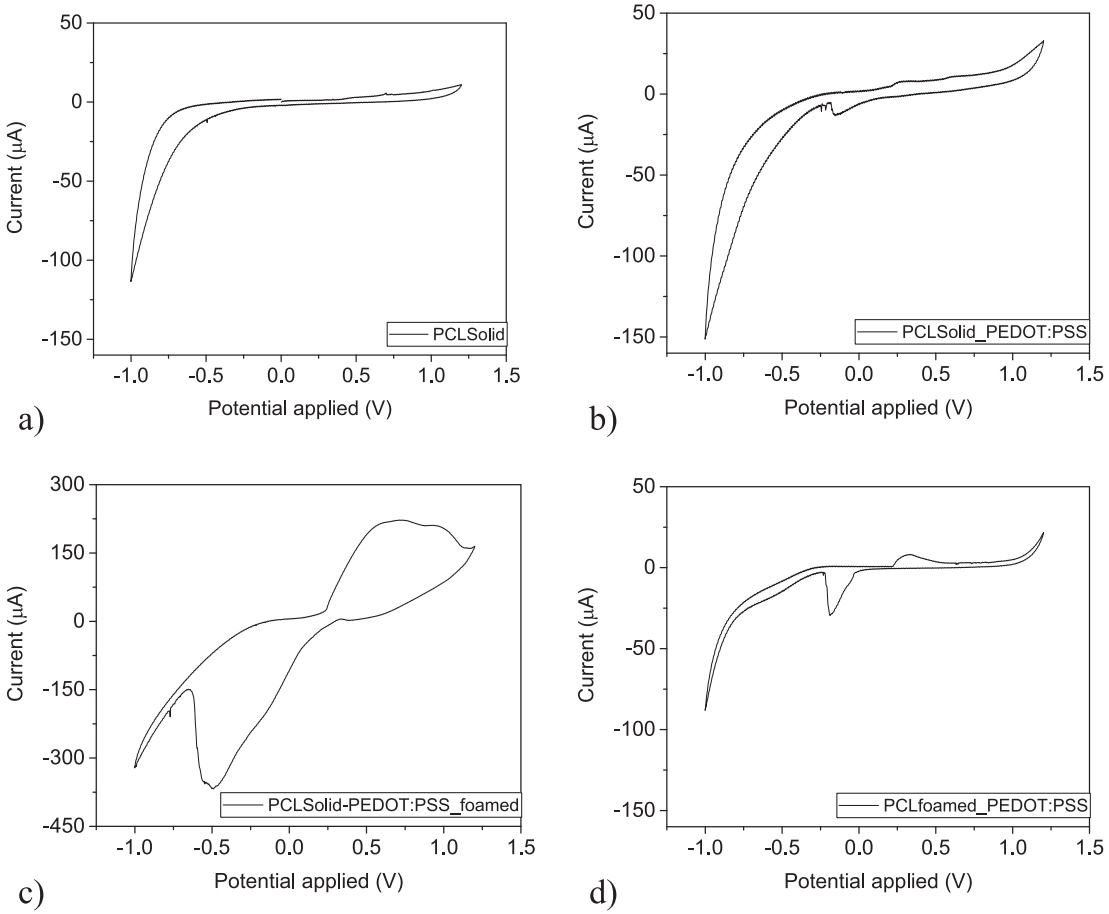

Fig. 7. Representative cyclic voltammograms of the PCLSolid sensor **(a)**, PCLSolid_Pedot:PSS sensor **(b)**, PCLFoamed_PEDOT:PSS sensor **(c)**, and PCLSolid_PEDOT:PSS_Foamed sensor **(d)** immersed in in 0.1 mol·L^{-1} KCl at scan rate 100 mV/s.

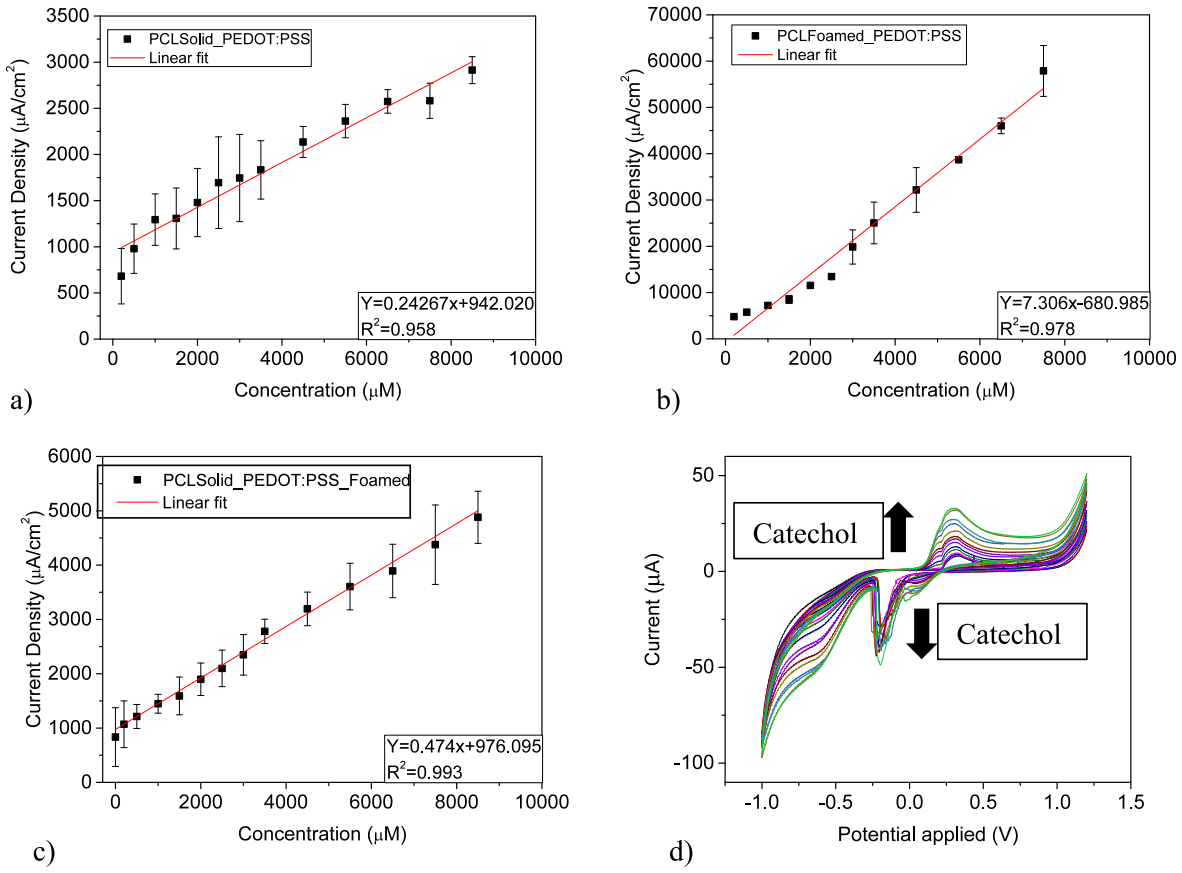

Fig. 8. Calibration curve when increasing the catechol concentration in KCl of the different sensors coated with PEDOT: PSS, PCLSolid_PEDOT:PSS **(a),** PCLFoamed_PEDOT:PSS sensor **(b)**, PCLSolid_PEDOT:PSS_Foamed **(c)** and cyclic voltammograms of the PCLSolid_PEDOT:PSS_Foamed sensor with different concentration of catechol **(d)**.

The addition of catechol produces the expected well-formed redox pair generated by the oxidation/reduction of two electrons of *ortho*-dihydroquinone to benzoquinone [54], (see Fig. 8**d**). However, a shift of the peaks is observed, as well as an increase in the intensity of the response in the coated samples, directly related to the concentration of catechol employed (Fig. 8**d**). First, it is worth noting the linearity of the response of the three sensors coated with PEDOT:PSS to the catechol additions. In all cases, the linear fit presents R^2 values close to or greater than 0.96 (see Table 3), showing the developed sensors potentiality for being used as electrocatalytic sensors. Specifically, the PCLFoamed_PEDOT:PSS sensor provides an electrocatalytic reaction towards catechol with good reversibility and a direct response with the concentration. Then, the stability of the PEDOT:PSS coating after the electrochemical study was checked. The diameter and surface morphology of the fibers before and after remained rather constant, indicating the stability of the fibers (see Supporting Information, section S3). Moreover, Raman studies confirmed the stability of the PEDOT:PSS coating (see Supporting Information, section S3).

3.2.1.2. Sensitivity, reproducibility, repeatability, and stability. Table 3 summarizes the results achieved for the four sensors developed, showing their response's linearity, sensitivity, and the theoretical limit of detection (LOD). Based on these results, it can be concluded that the fiber foaming process improves the sensitivity of the sensors in all cases, with PCLFoamed_PEDOT:PSS being particularly noteworthy (fibers first foamed and then coated with PEDOT: PSS), which has an increase of sensitivity of 30 times regarding those of PCLSolid_PEDOT:PSS (PEDOT: PSS coated solid fibers). Additionally, compared with other previously reported sensors for catechol detection, the PCLFoamed_PEDOT:PSS sensors also exhibited excellent electrocatalytic performance with a wide linear range up to 7500 μM, while previous works only reached up to 500 μM at the most [53,54,57].

Table 3
Response of the sensing capacity of the different sensors.

Muestra	R^2	Sensitivity (μA/μM)	LOD (M)
PCLSolid	–	0	0
PCLSolid_PEDOT:PSS	0.958	0.24	$1.48 \bullet 10^{-03}$
PCLFoamed_PEDOT:PSS	0.978	7.31	$3.93 \bullet 10^{-04}$
PCLSolid_PEDOT:PSS_Foamed	0.993	0.47	$1.27 \bullet 10^{-04}$

The performance of the PCLFoamed_PEDOT:PSS sensor, as previously explained, is related to the higher surface area provided by the foamed PCL fibers employed as a substrate, as well as to the higher amount of PEDOT:PSS transferred to the fibers (about 35–40 wt.%). On the contrary, the PCLSolid_PEDOT:PSS_Foamed sensor, which presents the same amount of PEDOT:PSS than the PCLSolid_PEDOT:PSS (about 20–25 wt.%), increases its sensitivity by a factor 2 regarding the PCLSolid_PEDOT:PSS sensor, and presents the lowest LOD of all the sensors, as well as the higher linearity. Once again, the foaming procedure provides a remarkable performance enhancement for the development of the sensors.

Additionally, the reproducibility of the sensors was examined by the cycling of at least five electrodes prepared using each procedure, being the variation coefficient in both cathodic and anodic peaks less than 1 % for the PCLSolid_PEDOT:PSS_Foamed sensor, while the other sensors coated by PEDOT:PSS showed a higher variability (see Supporting Information, section S4). Therefore, it was found that the production route carrying out the foaming procedure after the coating with PEDOT:PSS is highly reproducible, probably due to the recombination between the

PCL and PEDOT:PSS during the foaming procedure. In addition, the PCLSolid_PEDOT:PSS_Foamed sensors were selected due to its homogeneity to analyze the stability of their response, by performing repetitive measurements over the 10 cycles previously reached. It was found that it is possible to use the PCLSolid_PEDOT:PSS_Foamed sensors at least up to 50 cycles, obtaining only a decrease in intensity of less than 10 % (see Supporting Information, Fig. S8**d**). It can be highlighted that interfacial delamination of PEDOT:PSS coating layers due to the swelling of the PSS segments in presence of water is a common drawback of this kind of devices [31], particularly in absence of interactions between the coating and the substrate [58]. However, the developed sensors successfully overcome this limitation, as evidence both by Raman measurements and repetitive voltammetric measurements up to 50 cycles. This remarkable result can be related to the existence of interaction between the PEDOT:PSS coating and the PCL fibers that anchor the thin conductive coating layer to the substrate.

4. Conclusions

This work successfully proposes a new approach, based on an enhanced gas dissolution foaming route, to produce PCL-PEDOT:PSS fiber mats-based electrochemical sensors from solid electrospun PCL fiber mats. The insulation behaviour of the PCL was successfully overcome by the functionalization of the PCL fiber mats with PEDOT:PSS, a conductive polymer applied by a simple dip-coating procedure capable of transferring between 20 and 35 wt.% of PEDOT:PSS to the fiber mats, depending on the morphology of the initial fibers. Remarkably, the PEDOT:PSS is homogeneously distributed along the fibers mats as a thin coating layer of hundreds of nanometers around each individual fiber. In addition, PCL fibers already coated with PEDOT:PSS were successfully foamed, reaching equivalent expanded diameter and hollow structure that those foamed without the coating. Also, the PEDOT:PSS was found not only on the external surfaces of these fibers, but also on the inner porosity, evidencing that during the foaming procedure the PEDOT:PSS coating infused into the fibers, achieving an enhanced distribution both within the fiber mats and the individual fibers.

Then, the characterization of the four potential sensors developed, PCL solid fiber mats (PCLSolid), PCL solid fiber mats coated with PEDOT:PSS (PCLSolid_PEDOT:PSS), PCL foamed fiber mats coated with PEDOT:PSS (PCLFoamed_PEDOT:PSS), and PCL fiber mats foamed after being coated with PEDOT:PSS (PCLSolid_PEDOT:PSS_Foamed) by cyclic voltammetry evidenced the superior performance of the foamed fibers. It can be highlighted the enhanced response of the PCLSolid_PEDOT:PSS_Foamed sensor, which provided the higher linearity and lowest LOD for the detection of catechol, as well as two times higher sensitivity than the PCLSolid_PEDOT:PSS sensor. Moreover, the measurements performed with this sensor proved to be repeatable up to 50 cycles with a decrease of intensity less than 10 %. Finally, the study of the sensors by EIS confirmed the superior features achieved by foaming the sensors by enhancing the adhesion of PEDOT:PSS to the PCL surfaces. In addition, the PCLSolid_PEDOT:PPS_Foamed sensor achieved a significant decrease in the resistance to electronic transfer, presenting enhanced features for their use in sensoring applications that can be related to both its higher surface area and the presence of PEDOT:PSS within the fibers, instead of only in their surfaces.

CRediT authorship contribution statement

Suset Barroso-Solares: Conceptualization, Methodology, Investigation, Writing – original draft. **Javier Pinto:** Conceptualization, Writing – review & editing. **Coral Salvo-Comino:** Methodology, Investigation. **Daniel Cuadra-Rodriguez:** Investigation. **Cristina Garcia-Cabezon:** Methodology, Investigation, Writing – review & editing. **Miguel Angel Rodriguez-Perez:** Resources, Supervision. **Maria Luz Rodriguez-Mendez:** Conceptualization, Resources, Supervision, Project administration, Funding acquisition, Writing – review & editing.

Declaration of Competing Interest

The authors declare the following financial interests/personal relationships which may be considered as potential competing interests: [Miguel Angel Rodriguez Perez, Maria Luz Rodriguez Mendez, Daniel Cuadra-Rodriguez, Javier Pinto reports financial support was provided by Ministry of Science Technology and Innovations. Miguel Angel Rodriguez Perez, Maria Luz Rodriguez Mendez, Cristina Garcia-Cabezon reports financial support was provided by Government of Castile and León. Suset Barroso-Solares reports financial support was provided by Government of Castile and León].

Data availability

Data will be made available on request.

Acknowledgments

Financial assistance from Ministerio de Ciencia e Innovación (Spain) (PID2021-127108OB-I00 and FPI grant: PRE2019-088820), MCIN/AEI /10.13039/501100011033 and the EU NextGenerationEU/ PRTR program (PLEC2021-007705), Ministerio de Ciencia, Innovación y Universidades (MCIU) (Spain), FEDER "Una manera de hacer Europa" (EU) (RTI2018 - 098749-B-I00 and RTI2018 - 097367-A-I00), Regional Government of Castilla y León and the EU-FEDER program (CLU-2019-04, VA275P18, and VA202P20) are gratefully acknowledged. Also, we appreciate the financial support of MINECO-FEDER Plan Nacional (PID2021-122365OB-100). Junta de Castilla y Leon- FEDER VA202P20. CLU-2019-04 and «Infraestructuras Red de Castilla y León (INFRARED)» UVA01. Plan Tractor En Materiales Avanzados Enfocado A Los Sectores Industriales Claves En Castilla Y León: Agroalimentario, Transporte, Energía Y Construcción (MA2TEC).

Appendix A. Supplementary data

Supplementary data to this article can be found online at https://doi.org/10.1016/j.apsusc.2023.158062.

References

[1] M. Abrisham, M. Noroozi, M. Panahi-Sarmad, M. Arjmand, V. Goodarzi, Y. Shakeri, H. Golbaten-Mofrad, P. Dehghan, A. Seyfi Sahzabi, M. Sadri, L. Uzun, The role of polycaprolactone-triol (PCL-T) in biomedical applications: A state-of-the-art review, Eur. Polym. J. 131 (2020) 109701, https://doi.org/10.1016/j.eurpolymj.2020.109701.

[2] S. Barroso-Solares, D. Cuadra-Rodriguez, M.L. Rodriguez-Mendez, M.A. Rodriguez-Perez, J. Pinto, A new generation of hollow polymeric microfibers produced by gas dissolution foaming, J. Mater. Chem. B. 8 (2020) 8820–8829, https://doi.org/10.1039/D0TB01560A.

[3] R. Dwivedi, S. Kumar, R. Pandey, A. Mahajan, D. Nandana, D.S. Katti, D. Mehrotra, Polycaprolactone as biomaterial for bone scaffolds: Review of literature, J. Oral Biol. Craniofac. Res. 10 (2020) 381–388, https://doi.org/10.1016/j.jobcr.2019.10.003.

[4] H.S. Abdo, A.A. Elzatahry, H.F. Alharbi, K.A. Khalil, Electrical Conductivity Behavior of Biopolymer Composites, in: K.K. Sadasivuni, D. Ponnamma, J. Kim, J.-J. Cabibihan, M.A. AlMaadeed (Eds.), Biopolymer Composites in Electronics, Elsevier, 2017: pp. 13–25. 10.1016/B978-0-12-809261-3.00002-4.

[5] M. Mirjalili, S. Zohoori, Review for application of electrospinning and electrospun nanofibers technology in textile industry, J. Nanostructure Chem. 6 (2016) 207–213, https://doi.org/10.1007/s40097-016-0189-y.

[6] S. Barroso-Solares, J. Pinto, G. Nanni, D. Fragouli, A. Athanassiou, Enhanced oil removal from water in oil stable emulsions using electrospun nanocomposite fiber mats, RSC Adv. 8 (2018) 7641–7650, https://doi.org/10.1039/C7RA12646H.

[7] H. Tu, D. Li, Y. Yi, R. Liu, Y. Wu, X. Dong, X. Shi, H. Deng, Incorporation of rectorite into porous polycaprolactone/TiO2 nanofibrous mats for enhancing photocatalysis properties towards organic dye pollution, Compos. Commun. 15 (2019) 58–63, https://doi.org/10.1016/j.coco.2019.06.006.

[8] A. Luzio, E.V. Canesi, C. Bertarelli, M. Caironi, Electrospun polymer fibers for electronic applications, Materials. 7 (2014) 906–947, https://doi.org/10.3390/ma7020906.

[9] M. Ravi, S. Song, K. Gu, J. Tang, Z. Zhang, Electrical properties of biodegradable poly(ε-caprolactone): Lithium thiocyanate complexed polymer electrolyte films, Mater. Sci. Eng. B. 195 (2015) 74–83, https://doi.org/10.1016/j.mseb.2015.02.003.

[10] A. Lari, N. Sultana, C. Fhong Soon, Biocomposites conductive scaffold based on PEDOT:PSS/nHA/chitosan/PCL: Fabrication and characterization, Mal. J. Fund. Appl. Sci. 15 (2019) 146–149, https://doi.org/10.11113/mjfas.v15n2.1201.

[11] J. Yan, M. Li, Z. Wang, C. Chen, C. Ma, G. Yang, Highly tough, multi-stimuli-responsive, and fast self-healing supramolecular networks toward strain sensor application, Chem. Eng. J. 389 (2020) 123468, https://doi.org/10.1016/j.cej.2019.123468.

[12] Z. Wang, Y. Ying, L. Li, T. Xu, Y. Wu, X. Guo, F. Wang, H. Shen, Y. Wen, H. Yang, Stretched graphene tented by polycaprolactone and polypyrrole net–bracket for neurotransmitter detection, Appl. Surf. Sci. 396 (2017) 832–840, https://doi.org/10.1016/j.apsusc.2016.11.038.

[13] X.X. Wang, G.F. Yu, J. Zhang, M. Yu, S. Ramakrishna, Y.Z. Long, Conductive polymer ultrafine fibers via electrospinning: Preparation, physical properties and applications, Prog. Mater. Sci. 115 (2021) 100704, https://doi.org/10.1016/j.pmatsci.2020.100704.

[14] J.V. Patil, S.S. Mali, A.S. Kamble, C.K. Hong, J.H. Kim, P.S. Patil, Electrospinning: A versatile technique for making of 1D growth of nanostructured nanofibers and its applications: An experimental approach, Appl. Surf. Sci. 423 (2017) 641–674, https://doi.org/10.1016/j.apsusc.2017.06.116.

[15] K. Aruchamy, A. Mahto, S.K. Nataraj, Electrospun nanofibers, nanocomposites and characterization of art: Insight on establishing fibers as product, Nano-Struct. Nano-Objects. 16 (2018) 45–58, https://doi.org/10.1016/j.nanoso.2018.03.013.

[16] M. Bassyouni, M.H. Abdel-Aziz, M.S. Zoromba, S.M.S. Abdel-Hamid, E. Drioli, A review of polymeric nanocomposite membranes for water purification, J. Ind. Eng. Chem. 73 (2019) 19–46, https://doi.org/10.1016/j.jiec.2019.01.045.

[17] A. Bhatnagar, M. Sillanpää, A review of emerging adsorbents for nitrate removal from water, Chem. Eng. J. 168 (2011) 493–504, https://doi.org/10.1016/j.cej.2011.01.103.

[18] F. Wang, K. Liu, Y. Xi, Z. Li, One-step electrospinning PCL/ph-LPSQ nanofibrous membrane with excellent self-cleaning and oil-water separation performance, Polymer (Guildf). 249 (2022) 124858, https://doi.org/10.1016/J.POLYMER.2022.124858.

[19] G. Liu, X. Chen, J. Liu, C. Liu, J. Xu, Q. Jiang, Y. Jia, F. Jiang, X. Duan, P. Liu, Fabrication of PEDOT:PSS/rGO fibers with high flexibility and electrochemical performance for supercapacitors, Electrochim. Acta. 365 (2021) 137363, https://doi.org/10.1016/j.electacta.2020.137363.

[20] X. Liu, K. Li, C. Hou, H. Li, P. Chen, Q. Zhang, Y. Li, H. Wang, Poly-ε-caprolactone nanofibrous mats as electrolyte host for tailorable flexible electrochromic devices, Mater. Sci. Eng. B. 241 (2019) 36–41, https://doi.org/10.1016/j.mseb.2019.02.001.

[21] S. Vandghanooni, M. Eskandani, Natural polypeptides-based electrically conductive biomaterials for tissue engineering, Int. J. Biol. Macromol. 147 (2020) 706–733, https://doi.org/10.1016/j.ijbiomac.2019.12.249.

[22] D.J. Yun, J. Jung, K.H. Kim, H. Ra, J.M. Kim, B.S. Choi, J. Jang, M. Seol, Y.J. Jeong, Simultaneous increases in electrical conductivity and work function of ionic liquid treated PEDOT:PSS: In-depth investigation and thermoelectric application, Appl. Surf. Sci. 553 (2021) 149584, https://doi.org/10.1016/j.apsusc.2021.149584.

[23] I. Song, N. Yeon Park, G. Seung Jeong, J. Hwan Kang, J. Hwa Seo, J.Y. Choi, Conductive channel formation for enhanced electrical conductivity of PEDOT:PSS with high work-function, Appl. Surf. Sci. 529 (2020) 147176, https://doi.org/10.1016/j.apsusc.2020.147176.

[24] Y.J. Jo, S.Y. Kim, J.H. Hyun, B. Park, S. Choy, G.R. Koirala, T. il Kim, Fibrillary gelation and dedoping of PEDOT:PSS fibers for interdigitated organic electrochemical transistors and circuits, npj Flex, Electron. 6 (2022) 31, https://doi.org/10.1038/s41528-022-00167-7.

[25] A.F. al Naim, A.G. El-Shamy, Review on recent development on thermoelectric functions of PEDOT:PSS based systems, Mater. Sci. Semicond. Process. 152 (2022) 107041, https://doi.org/10.1016/j.mssp.2022.107041.

[26] B. Bessaire, M. Mathieu, V. Salles, T. Yeghoyan, C. Celle, J.P. Simonato, A. Brioude, Synthesis of continuous conductive PEDOT: PSS nanofibers by electrospinning: A conformal coating for optoelectronics, ACS Appl. Mater. Interfaces. 9 (2017) 950–957, https://doi.org/10.1021/acsami.6b13453.

[27] G. De Alvarenga, B.M. Hryniewicz, I. Jasper, R.J. Silva, V. Klobukoski, F.S. Costa, T.N.M. Cervantes, C.D.B. Amaral, J.T. Schneider, L. Bach-Toledo, P. Peralta-Zamora, T.L. Valerio, F. Soares, B.J.G. Silva, M. Vidotti, Recent trends of micro and nanostructured conducting polymers in health and environmental applications, J. Electroanal. Chem. 879 (2020) 114754, https://doi.org/10.1016/j.jelechem.2020.114754.

[28] A. Dominguez-Alfaro, M. Criado-Gonzalez, E. Gabirondo, H. Lasa-Fernández, J. L. Olmedo-Martínez, N. Casado, N. Alegret, A.J. Müller, H. Sardon, A. Vallejo-Illarramendi, D. Mecerreyes, Electroactive 3D printable poly(3,4-ethylenedioxythiophene)-graft-poly(ε-caprolactone) copolymers as scaffolds for muscle cell alignment, Polym. Chem. 13 (2022) 109–120, https://doi.org/10.1039/D1PY01185E.

[29] J. Yin, Y. Bai, J. Lu, J. Ma, Q. Zhang, W. Hong, T. Jiao, Enhanced mechanical performances and high-conductivity of rGO/PEDOT:PSS/PVA composite fiber films via electrospinning strategy, Colloids Surf. A: Physicochem. Eng. Asp. 643 (2022) 128791, https://doi.org/10.1016/j.colsurfa.2022.128791.

[30] L. Ferlauto, P. Vagni, A. Fanelli, E.G. Zollinger, K. Monsorno, R.C. Paolicelli, D. Ghezzi, All-polymeric transient neural probe for prolonged in-vivo electrophysiological recordings, Biomaterials. 274 (2021) 120889, https://doi.org/10.1016/J.BIOMATERIALS.2021.120889.

[31] M. Modarresi, A. Mehandzhiyski, M. Fahlman, K. Tybrandt, I. Zozoulenko, Microscopic understanding of the granular structure and the swelling of PEDOT:PSS, Macromolecules. 53 (2020) 6267–6278, https://doi.org/10.1021/acs.macromol.0c00877.

[32] X. He, J. Shi, Y. Hao, L. Wang, X. Qin, J. Yu, PEDOT:PSS/CNT composites based ultra-stretchable thermoelectrics and their application as strain sensors, Compos. Commun. 27 (2021) 100822, https://doi.org/10.1016/J.COCO.2021.100822.

[33] Q. Lei, J. He, D. Li, Electrohydrodynamic 3D printing of layer-specifically oriented, multiscale conductive scaffolds for cardiac tissue engineering, Nanoscale. 11 (2019) 15195–15205, https://doi.org/10.1039/c9nr04989d.

[34] D. Iandolo, A. Ravichandran, X. Liu, F. Wen, J.K.Y. Chan, M. Berggren, S.H. Teoh, D.T. Simon, Development and characterization of organic electronic scaffolds for bone tissue engineering, Adv. Healthc. Mater. 5 (2016) 1505–1512, https://doi.org/10.1002/ADHM.201500874.

[35] Y. Tian, Z. Wang, L. Wang, Hollow fibers: From fabrication to applications, Chem. Commun. 57 (2021) 9166–9177, https://doi.org/10.1039/d1cc02991f.

[36] V. Kumar, N.P. Suh, A process for making microcellular thermoplastic parts, Polym. Eng. Sci. 30 (1990) 1323–1329, https://doi.org/10.1002/pen.760302010.

[37] F.F.A. Martini-Vvedensky, J.J.E. Suh, N.N.P. Waldman, Microcellular closed cell foams and their method of manufacture, US 4473665 A (1982). https://lens.org/081-916-146-865-196.

[38] M.D. Abràmoff, P.J. Magalhães, S.J. Ram, Image processing with imageJ, Biophotonics Int. 11 (2004) 36–41, https://doi.org/10.1117/1.3589100.

[39] M.R. Moraes, A.C. Alves, F. Toptan, M.S. Martins, E.M.F. Vieira, A.J. Paleo, A. P. Souto, W.L.F. Santos, M.F. Esteves, A. Zille, Glycerol/PEDOT:PSS coated woven fabric as a flexible heating element on textiles, J. Mater. Chem. C: Mater. 5 (2017) 3807–3822, https://doi.org/10.1039/C7TC00486A.

[40] D. Antiohos, G. Folkes, P. Sherrell, S. Ashraf, G.G. Wallace, P. Aitchison, A. T. Harris, J. Chen, A.I. Minett, Compositional effects of PEDOT-PSS/single walled carbon nanotube films on supercapacitor device performance, J. Mater. Chem. 21 (2011) 15987, https://doi.org/10.1039/c1jm12986d.

[41] Y. Ren, L. Qing, L. Li, H. Hasichaolu, K.O. Zheng, Facile synthesis of highly conductive polymer fiber for application in flexible fringing field capacitive sensor, Sens. Actuators A: Phys. 342 (2022) 113616, https://doi.org/10.1016/j.sna.2022.113616.

[42] L.M. Lozano-Sánchez, I. Bagudanch, A.O. Sustaita, J. Iturbe-Ek, L.E. Elizalde, M. L. Garcia-Romeu, A. Elías-Zúñiga, Single-point incremental forming of two biocompatible polymers: An insight into their thermal and structural properties, Polymers (Basel). 10 (2018) 391, https://doi.org/10.3390/polym10040391.

[43] D. Li, Y. Xia, Electrospinning of nanofibers: Reinventing the wheel? Adv. Mat. 16 (2004) 1151–1170, https://doi.org/10.1002/adma.200400719.

[44] R. Ekambaram, M. Sugumar, S. Karuppasamy, P. Prasad, S. Dharmalingam, Fabrication of wheatgrass incorporated PCL/chitosan biomimetic nanoscaffold for skin wound healing: In vitro and In silico analysis, J. Drug Deliv. Sci. Technol. 71 (2022) 103286, https://doi.org/10.1016/j.jddst.2022.103286.

[45] J. Lee, W. Choi, Surface modification of sulfur cathodes with PEDOT:PSS conducting polymer in lithium-sulfur batteries, J. Electrochem. Soc. 162 (2015) A935, https://doi.org/10.1149/2.0651506jes.

[46] Z. Lian, S.A. Epstein, C.W. Blenk, A.D. Shine, Carbon dioxide-induced melting point depression of biodegradable semicrystalline polymers, J. Supercrit. Fluids. 39 (2006) 107–117, https://doi.org/10.1016/j.supflu.2006.02.001.

[47] B. Rossi, C. de Menezes, I. Thaís, L. Do, A. Montanheiro, A. Da, G. Sampaio, I. Cristiane, Y. Koga-Ito, I. Gilmar, P. Thim, I. Larissa, S. Montagna, PCL/β-AgVO 3 nanocomposites obtained by solvent casting as potential antimicrobial biomaterials, J. Appl. Polym. Sci. (2020) 50130, https://doi.org/10.1002/app.50130.

[48] V. Mittal, T. Akhtar, G. Luckachan, N. Matsko, PLA, TPS and PCL binary and ternary blends: Structural characterization and time-dependent morphological changes, Colloid Polym. Sci. 293 (2015) 573–585, https://doi.org/10.1007/s00396-014-3458-7.

[49] S.H. Chang, C.H. Chiang, F.S. Kao, C.L. Tien, C.G. Wu, Unraveling the enhanced electrical conductivity of PEDOT:PSS thin films for ITO-free organic photovoltaics, IEEE Photonics J. 6 (2014) 8400307, https://doi.org/10.1109/JPHOT.2014.2331254.

[50] D. Jucius, A. Lazauskas, V. Grigaliunas, R. Gudaitis, A. Guobiene, I. Prosycevas, B. Abakeviciene, M. Andrulevicius, Structure and properties of Dual-doped PEDOT:PSS multilayer films, Mater. Res. 22 (2019), https://doi.org/10.1590/1980-5373-MR-2019-0134.

[51] X. Jiang, Z. Wang, W. Han, Q. Liu, S. Lu, Y. Wen, J. Hou, F. Huang, S. Peng, D. He, G. Cao, High performance silicon-organic hybrid solar cells via improving conductivity of PEDOT:PSS with reduced graphene oxide, Appl. Surf. Sci. 407 (2017) 398–404, https://doi.org/10.1016/j.apsusc.2017.02.193.

[52] J. Bobacka, A. Lewenstam, A. Ivaska, Electrochemical impedance spectroscopy of oxidized poly(3,4-ethylenedioxythiophene) film electrodes in aqueous solutions, J. Electroanal. Chem. 489 (2000) 17–27, www.elsevier.nl/locate/jelechem.

[53] C. García-Hernández, C. García-Cabezón, F. Martín-Pedrosa, J.A. de Saja, M. L. Rodríguez-Méndez, Layered composites of PEDOT/PSS/nanoparticles and PEDOT/PSS/phthalocyanines as electron mediators for sensors and biosensors, Beilstein J. Nanotechnol. 7 (2016) 1948–1959, https://doi.org/10.3762/bjnano.7.186.

[54] A.L. Soares, M.L. Zamora, L.F. Marchesi, M. Vidotti, Adsorption of catechol onto PEDOT films doped with gold nanoparticles: Electrochemical and spectroscopic studies, Electrochim. Acta. 322 (2019) 134773, https://doi.org/10.1016/j.electacta.2019.134773.

[55] M.A. Bhat, R.A. Rather, A.H. Shalla, PEDOT and PEDOT:PSS conducting polymeric hydrogels: A report on their emerging applications, Synth. Met. 273 (2021) 116709, https://doi.org/10.1016/j.synthmet.2021.116709.

[56] A.A. Arrieta, C. Apetrei, M.L. Rodriguez-Mendez, J.A. de Saja, Voltammetric sensor array based on conducting polymer-modified electrodes for the discrimination of

liquids, Electrochim. Acta. 49 (2004) 4553–4561, https://doi.org/10.1016/j.electacta.2004.04.039.
[57] Y. Qian, C. Ma, S. Zhang, J. Gao, M. Liu, K. Xie, S. Wang, K. Sun, H. Song, High performance electrochemical electrode based on polymeric composite film for sensing of dopamine and catechol, Sens. Actuators B: Chem. 255 (2018) 1655–1662, https://doi.org/10.1016/j.snb.2017.08.174.
[58] Y. Wen, J. Xu, Scientific importance of water-processable PEDOT–PSS and Preparation, challenge and new application in sensors of its film electrode: A review, J. Polym. Sci. A: Polym. Chem. 55 (2017) 1121–1150, https://doi.org/10.1002/pola.28482.